

## RESEARCH ARTICLE

WILEY

# Mapping language with resting-state functional magnetic resonance imaging: A study on the functional profile of the language network

Paulo Branco<sup>1,2</sup>  | Daniela Seixas<sup>2</sup> | São L. Castro<sup>1</sup> 

<sup>1</sup>Centre for Psychology, University of Porto, Porto, Portugal

<sup>2</sup>Department of Biomedicine, University of Porto, Porto, Portugal

## Correspondence

Paulo Branco and São L. Castro, Faculty of Psychology and Educational Sciences, University of Porto, Rua Alfredo Allen, Porto 4200-135, Portugal.

Email: paulobranco@fpce.up.pt (P. B.) and slcastro@fpce.up.pt (S. L. C.)

## Funding information

Fundação para a Ciência e a Tecnologia, Grant/Award Numbers: SFRH/BD/86912/2012, UID/PSI/000050/2013

## Abstract

Resting-state functional magnetic resonance imaging (rsfMRI) is a promising technique for language mapping that does not require task-execution. This can be an advantage when language mapping is limited by poor task performance, as is common in clinical settings. Previous studies have shown that language maps extracted with rsfMRI spatially match their task-based homologs, but no study has yet demonstrated the direct participation of the rsfMRI language network in language processes. This demonstration is critically important because spatial similarity can be influenced by the overlap of domain-general regions that are recruited during task-execution. Furthermore, it is unclear which processes are captured by the language network: does it map rather low-level or high-level (e.g., syntactic and lexico-semantic) language processes? We first identified the rsfMRI language network and then investigated task-based responses within its regions when processing stimuli of increasing linguistic content: symbols, pseudowords, words, pseudosentences and sentences. The language network responded only to language stimuli (not to symbols), and higher linguistic content elicited larger brain responses. The left frontoparietal, the default mode, and the dorsal attention networks were examined and yet none showed language involvement. These findings demonstrate for the first time that the language network extracted through rsfMRI is able to map language in the brain, including regions subtending higher-level syntactic and semantic processes.

## KEYWORDS

brain mapping, functional connectivity, language network, presurgical planning, resting-state fMRI

## 1 | INTRODUCTION

Language mapping with functional magnetic resonance imaging (fMRI) is used in clinical settings to assist in presurgical planning and prevent the removal of eloquent cortex (Binder et al., 1997; Bookheimer, 2007; Stippich et al., 2007; Sunaert, 2006). This procedure is usually

implemented with task-based protocols in which the subject is asked to perform one or more language tasks inside the scanner (Binder, Swanson, Hammeke, & Sabsevitz, 2008; Sunaert, 2006). Due to clinical impairments, it is common that patients cannot perform the task optimally, and this can have a negative impact on the quality of the exam (Price, Crinion, & Friston, 2006). Furthermore, different clinically-tailored

This is an open access article under the terms of the Creative Commons Attribution-NonCommercial License, which permits use, distribution and reproduction in any medium, provided the original work is properly cited and is not used for commercial purposes.

© 2019 The Authors. *Human Brain Mapping* published by Wiley Periodicals, Inc.

task protocols can recruit different brain regions, and this may lead to undesirable inconsistency in the mapping results (Binder et al., 2008; Pillai & Zaca, 2011; Wilson, Bautista, Yen, Lauderdale, & Eriksson, 2017). Resting-state fMRI (rsfMRI) has recently been suggested as an alternative method to map language in the brain: it does not require task-execution nor intensive subject cooperation, and thus is appropriate to patients who are not good candidates for the conventional task-based protocol, including children, elderly, patients with language impairments and, arguably, patients under sedation (Branco et al., 2016; Sair et al., 2016; Tie et al., 2014).

Resting-state fMRI registers spontaneous hemodynamic fluctuations during rest that co-activate within functionally coupled regions, reflecting the underlying macrostructural organization of the brain (Biswal, Zerrin Yetkin, Haughton, & Hyde, 1995; Deco, Jirsa, & McIntosh, 2011; Fox & Raichle, 2007). Through methods such as seed-based correlation (Fox et al., 2005) or independent component analyses (Beckmann, DeLuca, Devlin, & Smith, 2005; Damoiseaux et al., 2006), patterns of co-activation can be identified, extracted and used to map well-known networks such as the fronto-parietal network (FPN), the default mode network (DMN) and the language network (Shirer, Ryali, Rykhlevskaia, Menon, & Greicius, 2011). Even though the subject is not performing a task, the obtained mapping results are replicable over time (Branco, Seixas, & Castro, 2018; Shehzad et al., 2009) and consistent across subjects (Damoiseaux et al., 2006), track major cognitive functions (Laird et al., 2011; Smith et al., 2009) and even predict individual task performance (Parker Jones, Voets, Adcock, Stacey, & Jbabdi, 2017; Tavor et al., 2016).

Previous studies have demonstrated that rsfMRI can map brain regions similar to those observed in language task-based protocols, both in healthy (Tie et al., 2014) and in clinical subjects (Branco et al., 2016; Sair et al., 2016). These regions mapped with rsfMRI have been attributed to language (the resting-state language network) by analyzing the spatial overlay with maps derived from task-based protocols. The assumption is that if the maps are spatially similar, they underpin the same cognitive processes. However, this approach is not entirely convincing because spatial overlay per se does not uncover which cognitive processes are actually being captured (Jackson, Cloutman, & Lambon Ralph, 2019). This is particularly relevant for language mapping because domain-general regions implicated in cognitive control, working-memory, and attention lie side by side with language-specific regions (Blank & Fedorenko, 2017; Fedorenko, Duncan, & Kanwisher, 2012; Geranmayeh, Wise, Mehta, & Leech, 2014; Humphreys & Lambon Ralph, 2014), and their recruitment during language tasks can affect the overlap results. Indeed, this approach has led to inconsistent reports on the functional role of resting-state networks, including the language network (Shirer et al., 2011; Smith et al., 2009). A case in point is the left FPN. It has been argued that the left FPN subtends language and, more generally, cognition (Laird et al., 2011; Smith et al., 2009). However, the left FPN has also been labeled as the executive network, while another network with adjacent non-overlapping regions is referred to as the language network (Shirer et al., 2011). Recent software for resting-state analyses (CONN functional connectivity toolbox, Whitfield-Gabrieli & Nieto-Castanon, 2012) segregates

the FPN and the language network, yet the left FPN is used as a proxy for language function in a number of studies (e.g., Smirnov et al., 2014; Zhu et al., 2014). It has also been argued the FPN can be separated into two left-lateralized networks (Geranmayeh et al., 2014), one that is domain-specific for language and another recruited by task-execution that is domain-general, but evidence regarding the specific role of regions found within the FPN, the language resting-state network, and their potential overlap remains scant.

Other well-known rsfMRI networks have been related to language, yet there is no account as to whether their involvement would be specific to language or not. One such case is the DMN, that has been attributed to semantic processing (Binder, Desai, Graves, & Conant, 2009; Seghier & Price, 2012). Evidence linking the DMN to semantic processing comes from studies that observed smaller task-induced deactivations in semantic compared to perceptual decision tasks and in hearing words versus pseudowords (Binder, Medler, Desai, Conant, & Liebenthal, 2005; Humphries, Binder, Medler, & Liebenthal, 2007), and from the observation of a partial spatial overlap between the DMN and the semantic system (Binder et al., 2009). At odds with these findings are others showing that the reduced deactivations for semantic tasks appear only in a small number of voxels within the left inferior parietal lobule whereas other regions have very heterogeneous functional profiles (Seghier & Price, 2012); other studies suggest that DMN deactivation can be attributed to task difficulty (McKiernan, Kaufman, Kucera-Thompson, & Binder, 2003; Esposito et al., 2009; but see Seghier & Price, 2012); and recent work shows distinct spatial and task-response profiles for multimodal semantic brain regions and the DMN (Jackson et al., 2019). So, the involvement of the DMN in language processing remains unclear. A similar appraisal applies to a subset of the multiple demand network that is known in the resting-state literature as the dorsal attention network, DAN (Fedorenko, Duncan, & Kanwisher, 2013; Geranmayeh, Chau, Wise, Leech, & Hampshire, 2017), and that is also recruited during the execution of language tasks (e.g., Fedorenko et al., 2013). Note, however, that this network is recruited in a wide range of cognitive tasks (Vossel, Geng, & Fink, 2013). A provisional conclusion from the findings reviewed above is that one should examine how each of these networks specifically responds to language, and determine if the rsfMRI language network captures language processes with a high degree of sensitivity and specificity before resting-state fMRI can be used to map language in clinical contexts.

One additional issue requiring clarification is that even if the rsfMRI language network is specifically implicated in language processing, it is currently unknown which processes it maps: is it low-level processes such as auditory decoding or phonological retrieval, or rather higher-level syntactic and lexico-semantic processes? Contemporary large-scale language models predict that separate brain systems – a dorsal and a ventral pathway comprising several brain regions along the frontal and temporal lobe coordinate to perform complex language computations such as syntax, semantics and phonology (Hickok & Poeppel, 2007; Saur et al., 2008). In this distributed language-network, brain regions not included in the classic language model also play an important role in language processing (Hagoort,

2014; Tremblay & Dick, 2016), including the supplementary motor area (SMA, Hertrich, Dietrich, & Ackermann, 2016; Lima, Krishnan, & Scott, 2016), the anterior temporal lobe (Jackson, Hoffman, Pobric, & Lambon Ralph, 2016; Ralph, Jefferies, Patterson, & Rogers, 2016), the middle frontal gyrus, the inferior temporal gyrus, and also homolog brain regions in the right hemisphere (Price, 2012 for an in-depth review). It has also been argued that language is best understood as a network rather than as an isolated set of highly-specialized brain regions (Fedorenko & Thompson-Schill, 2014), and this has been backed up by evidence that regions in the language network are structurally and functionally connected (Saur et al., 2008; Turken & Dronkers, 2011). This makes rsfMRI a suitable technique to explore the neural underpinnings of the language network. However, whether rsfMRI is able to target these functionally-relevant brain regions such that it can be applied in clinical settings remains a matter of debate. This is indeed a critical matter because the majority of studies comparing rsfMRI to task-based fMRI only show partial and moderate spatial overlap of the maps resulting from the two techniques (Branco et al., 2016; Sair et al., 2016; Tie et al., 2014). It is possible that, for example, rsfMRI only captures a subset of the functional language network, and this possibility should not be overlooked as the relevance of rsfMRI for presurgical planning depends on its ability to find eloquent brain regions that, if damaged, could lead to long-term deficits.

In this study, we investigate the functional profile of regions within the rsfMRI language network. Subjects will perform a rsfMRI protocol followed by a comprehensive task-based protocol that includes tasks with increasingly higher linguistic content. Subjects will visualize stimuli without linguistic content (non-linguistic symbols), and read stimuli with phonological information (pseudowords), phonological plus semantic information (words), phonology and syntax (pseudosentences), and phonological, semantic and syntactic information (sentences). Response profiles for these conditions will be examined at the group level for inferential purposes, and at the single-subject level to test the validity of this procedure in clinical settings. With this approach, we aim to clarify which processes are mapped within the rsfMRI language network. We will also explore the functional role of other networks that have been linked to language processing (left FPN, Smith et al., 2009), share spatial features with the language network (DMN, Binder et al., 2009), or take part in domain-general processing that—although recruited by language tasks—might not be language specific (DAN network, Fedorenko, 2014; Shirer et al., 2011). This will provide a deeper understanding of the resting-state language network, and will elucidate whether it can be considered a domain-specific network to be used with confidence for language mapping in presurgical planning.

## 2 | METHODS

### 2.1 | Participants

Sixteen adults took part in this experiment (seven male and nine female, mean age =  $25.6 \pm 3$ ). All were native speakers of European

Portuguese and right-handed according to the Edinburgh Handedness Test (Oldfield, 1971). Exclusion criteria were sight problems, neurological or neuropsychiatric diseases, and language or learning disorders. The study was conducted in accordance with the Declaration of Helsinki and approved by the local ethics committee (FMUP.17.07.2015). A brief explanation of the experiment was given and written informed consent was collected from all participants, who were told they could withdraw from the experiment at any time if they wished to (none did). Participants received a small monetary compensation for their time.

Sample size was estimated by calculating the number of subjects required for a statistical power equal or above 80%. This was done in a pilot study with an independent sample,  $N = 9$  (1 run per subject), using the tool *fmripower* (Mumford & Nichols, 2008). One-sample *t* tests were computed in the rsfMRI language network region-of-interest (ROI). For the high-level linguistic condition, sentences, 11 subjects were required for 80% power. We also examined statistical power within the task-responsive DAN network; all conditions had over 80% power with a sample size of 12 subjects. Power curves and additional information can be found in Figures S1 and S2.

### 2.2 | MRI acquisition

Subjects were scanned in a Siemens 3T Trio scanner with a 32 channel headcoil. Functional images were acquired using an EPI sequence with the following parameters: time of repetition (TR) = 2000 ms; time of echo (TE) = 30s; GRAPPA acceleration factor iPAT = 2; field of view (FOV) =  $192 \times 192 \text{ mm}^2$ ; flip angle =  $90^\circ$ ; slice thickness = 3.7 mm; in-plane pixel size  $2.7 \times 2.7 \text{ mm}^2$  and axial slices = 34. The first 8 s of acquisition in each run were excluded due to T1 equilibration effects. Temporal signal-to-noise ratio (tSNR) was calculated to ensure critical regions of interest (ROI) could capture changes in the bold response during task-execution (Jackson et al., 2016; Murphy, Bodurka, & Bandettini, 2007; Simmons, Reddish, Bellgowan, & Martin, 2009). To do so, for each voxel in the brain, the average of the signal over time was divided by its standard deviation, after motion correction and before other preprocessing steps. With the common exception of the ventral anterior temporal lobe and the medial prefrontal cortex, all regions showed appropriate tSNR (whole-brain tSNR maps can be inspected in Figure S3). A high-resolution T1 image was also acquired for registration purposes with the following parameters: TR = 2,530 ms; TE = 3.42 ms; GRAPPA acceleration factor iPAT = 2; FOV =  $256 \times 256 \text{ mm}^2$ ; flip angle =  $7^\circ$ ; slice thickness = 1 mm; in-plane pixel size  $1 \times 1 \text{ mm}^2$  and axial slices = 176.

### 2.3 | Resting-state fMRI procedure

Resting-state fMRI was acquired before task-based fMRI to ensure that the subjects were not influenced by, or thinking about, the task during rest. Subjects were instructed to lie still in the scanner with their eyes closed, to think of nothing in particular, and to avoid falling asleep. The resting-state protocol lasted 8 min.

## 2.4 | Task design, materials and procedure

The language task included five conditions composed of stimuli with increasingly higher linguistic content: non-linguistic symbol strings, pseudowords, words, pseudosentences and sentences. The rationale for this approach is that if the regions within the network are involved in language processes, then brain responses to the task will be increasing on par with the linguistic demand (Bedny, Pascual-Leone, Dodell-Feder, Fedorenko, & Saxe, 2011; Fedorenko et al., 2016). Importantly, as linguistically degraded stimuli require more reading effort than words and sentences (e.g., Bedny et al., 2011; Fedorenko, Hsieh, Nieto-Castañón, Whitfield-Gabrieli, & Kanwisher, 2010), a linear increase in brain responses to high-level linguistic content should not be due to a higher involvement of task-related general processes such as cognitive control, memory and attention. Materials for this task were selected as follows. First, a set of 72 European Portuguese two- and three-syllable words (mean number of letters = 5, range 4–6) were selected according to word frequency, imagery and concreteness using the online tool P-PAL (Soares et al., 2014). Words had medium to high frequency (mean =  $21.9 \pm 34.8$  occurrences per million), high imaginability ( $5.96 \pm 0.39$ , in a scale of 1–7), and high concreteness ratings ( $6.53 \pm 0.23$ , in a scale of 1–7). Pseudowords were then generated by replacing one to three phonemes in each word. To make sure that pseudowords were orthographically and phonologically valid, the bigram frequency of pseudowords was matched to that of the original word list ( $t = 1.06$ ,  $p = .29$ , *ns*). Non-linguistic symbols were created by converting each pseudoword to a symbol string using a false font from the Brussels Artificial Characters Sets (BACS2sans, Vidal, Content, & Chetail, 2017). This false font is matched with the

letters of the alphabet for complexity, symmetry, line intersections and number of strokes, and so it is appropriate to establish a visually-matched baseline with no linguistic information. Sentences were created by combining two content words from the word list with function words (e.g., “but,” “because”), one verb, and adjectives such that a syntactically valid and semantically meaningful relationship between words was achieved. Finally, pseudosentences were created by converting content words from each sentence into pseudowords while keeping function words intact; as a result, pseudosentences were semantically meaningless but retained the syntactic and phonological structure of the original sentence (e.g., Bedny et al., 2011; Castro & Lima, 2010). In the interest of ecological validity, sentences and pseudosentences had larger lengths than word and pseudoword lists (see below). This difference in length was kept to a minimum: mean number of letters for sentences and pseudosentences =  $34.08 \pm 3.7$ , mean number of letters for word and pseudoword lists =  $30 \pm 1.7$ . An example for each condition can be seen in Figure 1(a).

We used a probe detection task to maintain subjects' engagement throughout the experiment. This task has been successfully used for single-subject language mapping by Fedorenko et al. (2010). Figure 1(a) shows one example of a trial. Subjects viewed a set of six stimuli in quick succession (1,500 ms each), followed by two stimuli simultaneously presented on the screen (3,000 ms). One of the two stimuli had been presented in the preceding sequence, the other had not.

Subjects were instructed to view (symbols conditions) or covertly read (all remaining conditions) the stimulus sequence, and then select from the two alternatives the one that had been presented previously. They did so by pressing a two-button MRI-compatible controller, the

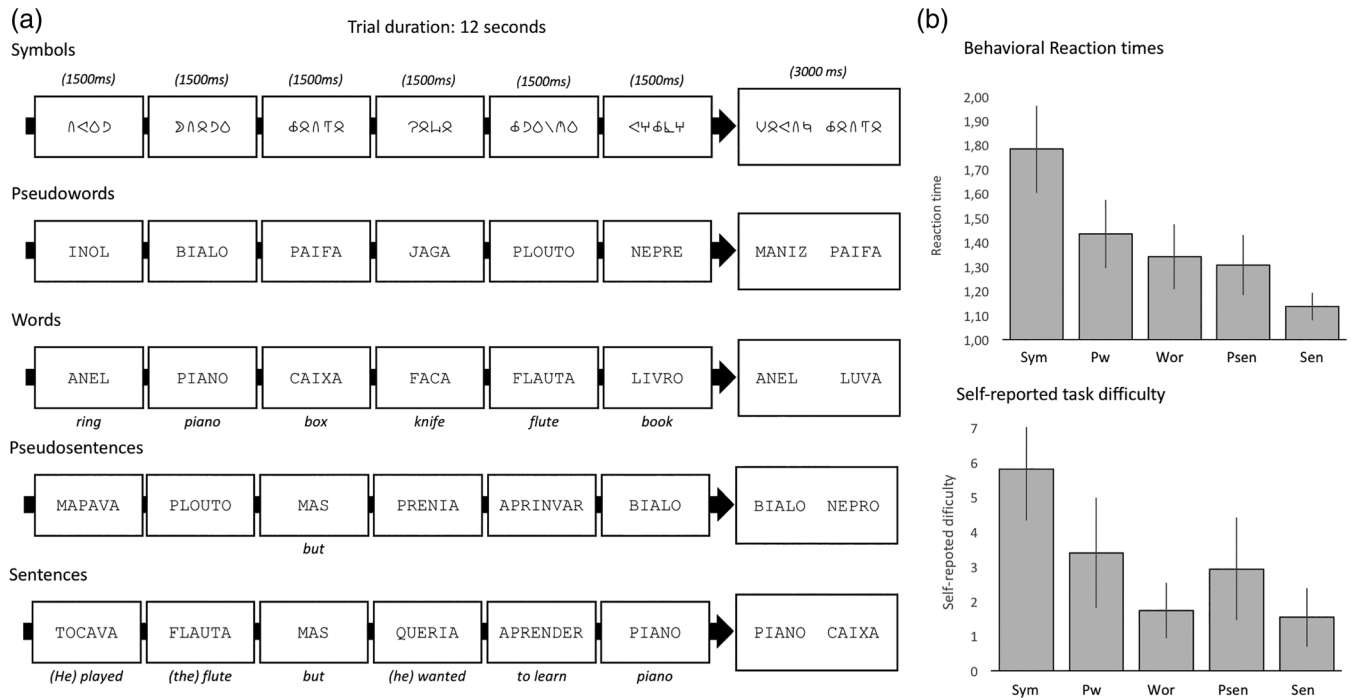


**FIGURE 1** (a) Example of an experimental trial for each condition. Six items are presented in quick succession followed by two alternatives. (b) Reaction times for each condition. Vertical bars denote 95% confidence intervals (c) Self-reported task difficulty (1–7, 1 = very easy; 7 = very hard). Vertical bars denote 95% confidence intervals

left one for the left stimulus, the right one for the right stimulus. The position of the correct probe was pseudorandomized and was presented at each side with equal odds (50%). Subjects were told to view/read the stimuli and refrain from using other strategies to aid in task performance. Before entering the scanner subjects ran a computer simulated version of the task to ensure that they understood the instructions and to familiarize themselves with the procedure.

To maximize fMRI signal detection, stimuli were presented using a block design with active periods of 24 s (two trials) alternating with 15 s of rest (fixation cross). Experimental conditions were presented in separate runs to avoid carryover and task-switching effects. A single run for one condition had six active and six rest periods and lasted for 4 min. Subjects performed two runs in each condition, for a combined acquisition time of 40 min (two runs, five conditions). The order of conditions and runs was counterbalanced across subjects following a balanced Latin square design.

Stimuli were presented in a 21-in. MRI compatible monitor at a visual angle of 3°–4° using the MATLAB plugin Psychtoolbox (version 3.0, Brainard, 1997). Subjects responded to the task using a two-button pad (Cedrus Lumina Response Box LP-400) connected to a Lumina 3G controller that recorded the button presses and corresponding reaction times. Eye-tracking was recorded throughout the experiment to monitor task compliance. After scanning, subjects filled a post-experiment survey where they rated the subjective difficulty of the task in each condition (1, very easy; 7, very hard). The whole experiment, including set-up, structural and functional acquisitions lasted 80 min.

## 2.5 | FMRI pre-processing

All analyses were performed using the Oxford Centre for Functional Magnetic Resonance Imaging of the Brain Software Library (FMRIB, Oxford, UK; FSL version 5.0.10). The same pre-processing pipeline was used for resting-state and task-based fMRI data: motion correction was performed using MCFLIRT (Jenkinson, Bannister, Brady, & Smith, 2002); non-brain tissue was removed with BET (Smith, 2002); spatial smoothing was applied using a 8 mm Full Width at Half Maximum (FWHM) Gaussian kernel; data were denoised using ICA-AROMA (Pruim et al., 2015); white matter and cerebral spinal fluid signals were estimated from the respective masks obtained with FAST (Zhang, Brady, & Smith, 2001), and were removed through multiple linear regression to eliminate any residual artifacts in the data; and data were temporally filtered using a high-pass filter at 80 and 100 seconds FWHM for task-based and rsfMRI, respectively. Finally, data were normalized to standard MNI space, first by warping functional data to structural space through FLIRT boundary-based registration (Jenkinson et al., 2002), and then by warping structural space data to standard MNI space using a linear transformation (FLIRT) with 12 degrees of freedom, further complemented with nonlinear registration (FNIRT, Andersson, Jenkinson, & Smith, 2007).

Exclusion criteria for excessive motion were peak displacements larger than 3.75 mm (voxel size), or average relative displacements larger than 0.5 mm. For rsfMRI, all protocols were included (average

relative displacement =  $0.06 \pm 0.06$  mm). For task-based fMRI, one subject had a peak displacement above 3.75 mm in one of the runs (pseudosentences condition, second run). Statistics for this condition were calculated using only the first, non-affected run. The remaining data had overall low motion indices (mean relative displacements of  $0.06 \pm 0.04$  mm).

## 2.6 | Resting-state analyses

Resting-state networks were extracted with independent component analysis (ICA). To do so, pre-processed data was analyzed using MELODIC multi-session temporal concatenation ICA (Beckmann & Smith, 2004). The number of extracted components was estimated with FSL default Laplacian approximation (Beckmann & Smith, 2004). Independent components (ICs) were thresholded using a mixture-model cut-off of 0.5 for an equal weight on false positives and false negatives (Woolrich, Behrens, Beckmann, & Smith, 2005). Group-level networks were then identified using a template matching procedure: the spatial overlap between each IC and a set of published group templates (Shirer et al., 2011) was calculated using the Dice coefficient (Rombouts, Barkhof, Hoogenraad, Sprenger, & Scheltens, 1998), and ICs were ranked according to the spatial similarity with networks of interest, from highest to lowest. The five highest ranked ICs for each network were visually inspected to confirm the accuracy of the procedure. The language, FPN and DMN networks were well characterized by one single IC. The DAN network was split into two mirrored ICs, left and right-lateralized, and both were identified by the template matching procedure as first- and second-ranked, respectively. The two ICs were combined to create a single DAN mask, considering that the original group template is bilaterally distributed (Shirer et al., 2011).

After template matching, the statistical threshold for each network was further adjusted by visual inspection to compensate for different network threshold cut-offs. Thresholds were selected such that the networks were visually similar to the templates used and included the major regions identified by Damoiseaux et al. (2006), Smith et al. (2009), and Shirer et al. (2011):  $z > 7$  for the language network;  $z > 6$  for the FPN;  $z > 5$  for the DMN; and  $z > 4$  for DAN network. For transparency, unthresholded maps can be consulted at NeuroVault.org (<https://neurovault.org/collections/SARZAHAW>). To better scrutinize the language network, a complementary region-of-interest (ROI) approach was used. To do so, statistical peak coordinates within each cluster were obtained using the FSL cluster tool. Then, each suprathreshold voxel within the network was assigned to a single ROI, according to the shortest Euclidean distance to each statistical peak. This resulted in a set of ROIs, one for each statistical peak.

Single-subject language networks were extracted with the same approach, but using single-session ICA MELODIC. Again, the resulting components were identified by template-matching and supplemented by visual inspection for quality assurance. After visual inspection, single-subject thresholds were fixed at  $z > 4$  for all subjects.

Finally, since ICA overfitting/underfitting can bias the network topography and impact the functional dissociation between rsfMRI

networks (Jackson et al., 2019), we examined the stability of the language network at different dimensionalities. To do so, group-level ICA analyses were further repeated with fixed dimensionalities, from 20 to 100 ICs, in steps of 10. Voxelwise correlations between the original IC, and the resulting ICs at each dimensionality, were performed as a way to quantify similarity and change as a consequence of ICA dimensionality.

## 2.7 | Task-protocol analyses

For task-based protocols, first-level analyses were conducted for each condition using FSL FEAT (FMRI Expert Analysis Tool, Smith et al., 2004). FILM pre-whitening was used on the EPI images and a simple contrast between block conditions convolved with the built-in double-gamma hemodynamic response function (HRF) was performed, also adding a first-order temporal derivative to compensate for single-subject HRF variability and slice-timing effects. The two acquired runs for each condition were then combined in higher-level fixed-effects GLM using a  $z > 3.1$  threshold and a Gaussian Field Theory corrected cluster  $p$  threshold of .05. To estimate the magnitude of brain responses for each condition, average percentage signal increases were estimated using FSL Featquery. This was performed using the network masks for the main analyses and individual ROIs for complementary ROI analyses. All statistical analyses were performed on percent signal change values.

## 3 | RESULTS

### 3.1 | Task performance

Button presses from five subjects in one of the scanning sessions were not correctly recorded due to a technical problem, and so RT and accuracy from these subjects were not analyzed, but all subjects filled the post-experiment survey (please note these responses are not critical to the task and were used only to examine task compliance and difficulty). For all conditions accuracy rates were well above chance (50%) showing that subjects performed the task efficiently: 76% correct for symbols, 95% for pseudowords, 97% for words, 97% for pseudosentences and 99% for sentences. We compared the reaction times of correct responses for each condition using a repeated measures ANOVA including all conditions in a single within-subjects factor, Task. Reaction times can be inspected in Figure 1(b). A main effect of Task showed significant differences between conditions ( $F(4, 40) = 55.33, p < .001, \eta_p^2 = .85$ ). Post-hoc analyses showed that symbols had slower reaction times than the four linguistic conditions (vs. pseudowords,  $p = .001$ ; vs. words, pseudosentences and sentences,  $ps < .001$ ). Other significant differences included slower reaction times for pseudowords compared to pseudosentences ( $p = .04$ ) and sentences ( $p < .001$ ). Sentences had the fastest reaction times compared to words and pseudosentences (all  $ps < .01$ ). In the post-experiment survey, subjects rated symbols as the hardest condition (mean = 5.8, range 1–7), followed by pseudowords and

pseudosentences (means of 3.4 and 2.9, respectively). Words and sentences were rated as the easiest conditions (means of 1.7 and 1.5, respectively, see Figure 1(b)).

### 3.2 | Resting-state network extraction and template matching

The resting-state language network was well identified (first ranked accordingly to the template matching algorithm), and was spatially similar to the language template used for classification (Dice = .24). The network contained several brain regions that are traditionally involved in language processing, including the inferior frontal gyrus, pars triangularis and opercularis; the posterior superior temporal gyrus; and the posterior middle temporal gyrus. The FPN, DMN and DAN were also successfully identified with the template matching procedure, with Dice values of 0.35 for the left FPN, 0.32 for the DMN, and 0.27 and 0.33 for the two ICs comprising the DAN network (left and right ICs, respectively). For a complete list of all clusters, statistical significance and MNI coordinates of the language network, please see Table 1. An overlap map of the classification templates with the rsfMRI networks can be seen in the Figure S4.

At the single-subject level, and for the language network, results were again consistent with the language template (mean Dice = 0.21, range 0.15–0.30) and, despite some individual variability, targeted classic language regions for all subjects. Regions of high convergence were the left IFG and the left superior and middle temporal gyri. The single-subject rsfMRI language maps for all subjects, as well as an intersubject probabilistic overlay map, are shown in Figure 2. They can also be consulted in NeuroVault.org (<https://neurovault.org/collections/SARZAHAW>).

Turning now to ICA dimensionality, we found no evidence of underfitting or overfitting close to the dimensionality automatically determined using the default MELODIC Laplacian estimation (original number of ICs = 52). Voxelwise correlations between the original language network, and the language network at dimensionalities between 20 and 70 were quite high ( $r > .70$ ), with no other competing IC exceeding an  $r > .30$ . In dimensionalities above 80, the language network started to split into two or more components, clustering the frontal and temporal brain regions separately (see Figure S5).

### 3.3 | Group-level results

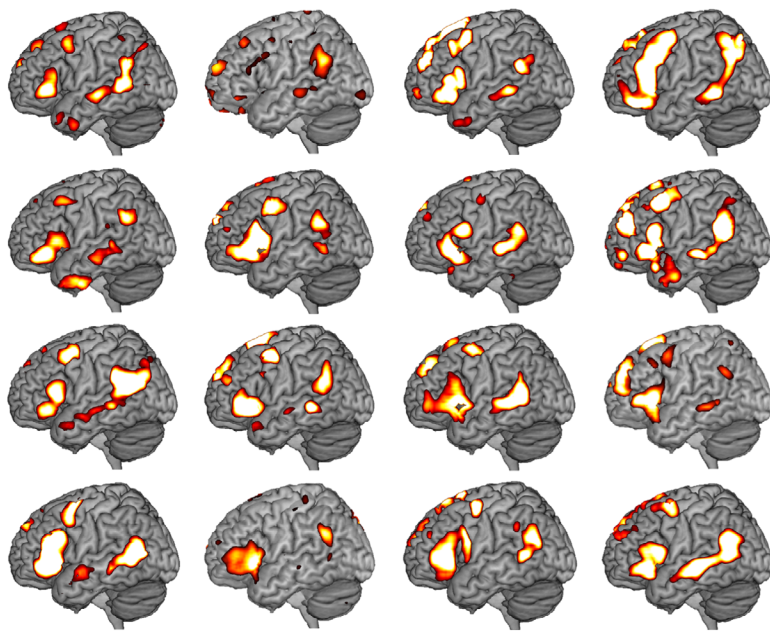
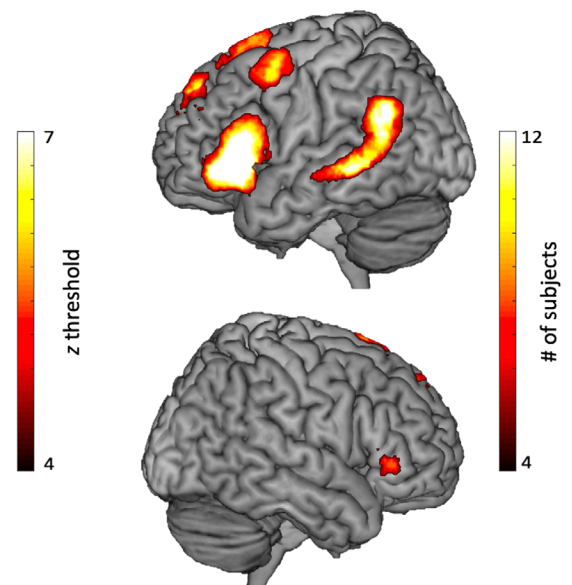
To test for differences in percent signal changes across conditions within the language network ROI, a repeated-measures ANOVA was calculated including all five conditions in a single within-subjects factor, Task. A main effect of Task was observed ( $F(1, 15) = 25.59, p < .001, \eta_p^2 = .63$ ). Further Bonferroni posthoc tests were conducted to examine pairwise differences. Of main interest here to highlight language involvement is the contrast between symbols (non-linguistic baseline) and each linguistic condition. Words ( $p = .013$ ), pseudosentences ( $p < .001$ ) and sentences ( $p < .001$ ) significantly differed from symbols (pseudowords,  $p = .34, ns$ ). Also, sentences and

**TABLE 1** Group-level results and MNI coordinates for the language network

Brain region	# voxels	MNI coordinates			z-Score
		x	y	z	
L posterior middle temporal gyrus	6,250	-56	-34	-2	18.3
L inferior frontal gyrus, pars triangularis		-50	28	-2	17.5
L middle temporal gyrus		-62	-44	6	16.1
L posterior supramarginal gyrus		-60	-50	10	15.9
L inferior frontal gyrus, pars opercularis		-54	18	18	15.1
L temporal pole		-54	6	-18	12.5
Superior frontal gyrus	425	-4	16	62	12.3
Superior frontal gyrus		-6	30	58	8.25
R posterior superior temporal gyrus	388	52	-36	2	10.7
Frontal pole	367	-8	48	42	12.3
L middle frontal gyrus	276	-42	4	56	10.6
R temporal pole	16	52	12	-18	7.49

Note: Labels taken from the Harvard-Oxford cortical atlas.

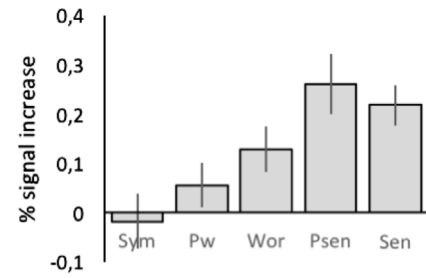
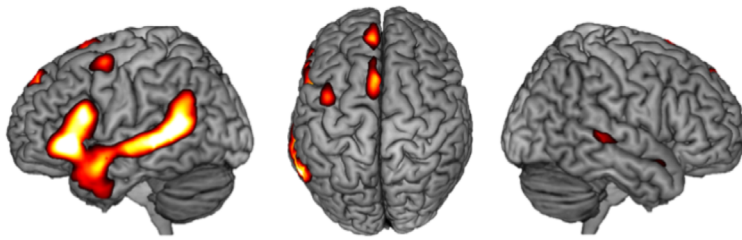
Abbreviations: L, Left; MNI, Montreal Neurological Institute; R, Right.

**(a)** Single-subject maps**(b)** Probabilistic overlay map**FIGURE 2** (a) Language network maps for all 16 subjects. (b) Probabilistic overlay map showing locations of high convergence across subjects. Cases 2, 12 and 14 had their minimum threshold set to  $z = 3$  for illustration purposes

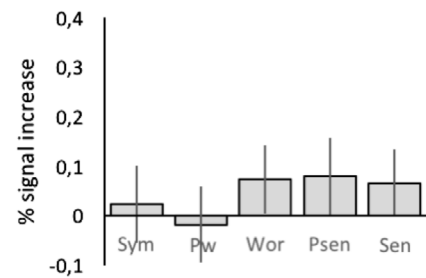
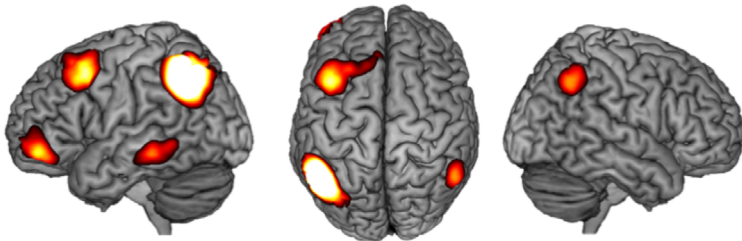
pseudosentences showed significantly higher percent signal change than words ( $p < .013$  for pseudosentences and  $p < .04$  sentences) but did not differ from each other (pseudosentences vs. sentences,  $p = 1$ , ns). Importantly, we expected to observe a linear increase in percent signal changes on par with the increase in linguistic content. To test this, we ran polynomial contrasts and examined the resulting model fits. We observed a significant linear model fit,  $F(1, 15) = 62.87$ ,  $p < .001$ ,  $\eta_p^2 = .81$ : conditions with higher linguistic content yielded higher percent signal changes (see Figure 3).

Additionally, we wanted to examine whether the five conditions showed significant activation during the task, that is, whether the percent signal changes differed from zero. We used a Bayesian approach to evaluate evidence for and against the null hypothesis (percent signal change  $> 0$ ) using JASP (JASP Team 2017). For this purpose, Bayesian one-sample t-tests were calculated for each condition (a Cauchy prior of .707 was used as default in JASP, Wagenmakers et al., 2017). The symbols condition had a Bayes factor ( $BF_{+0}$ ) of 0.17 indicative of moderate evidence in favor of the null hypothesis.

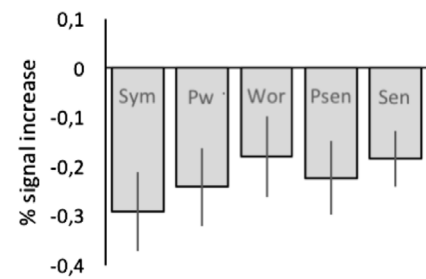
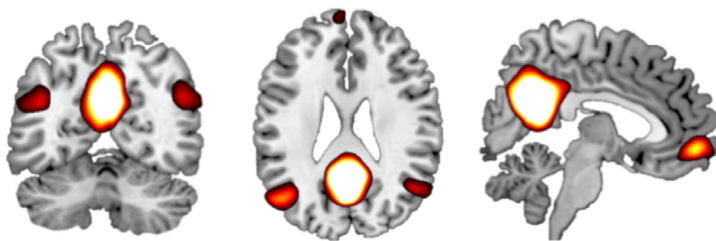
## (a) Language network



## (b) Fronto-parietal network



## (c) Default mode network



## (d) Dorsal attention network

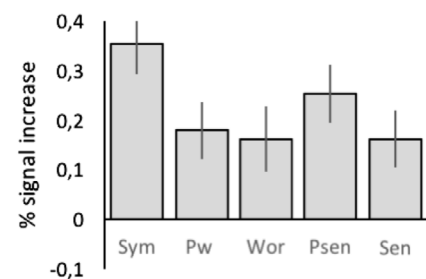
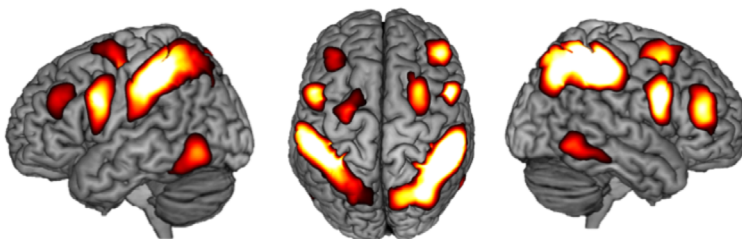


**FIGURE 3** Group-level resting-state functional magnetic resonance imaging networks and corresponding mean percent signal changes for each condition. Psen, pseudosentences; Pwor, pseudowords; Sen, sentences; Sym, symbols; Wor, words. Vertical bars denote 95% confidence intervals

Pseudowords had a  $BF_{+0}$  of 5.13, indicating moderate evidence in favor of alternative hypothesis. All the remaining conditions showed decisive evidence in favor of the alternative hypothesis, with  $BF_{+0} = 789.72$ ,  $BF_{+0} = 66,598.83$  and  $BF_{+0} = 840,668.69$  for words, pseudosentences and sentences, respectively.

To further characterize the language network, a comprehensive ROI analysis was performed by dividing the language network into 12 ROIs, each corresponding to a statistical peak coordinate. The

results from all statistical contrasts for the ROI analyses can be seen in Table 2. The majority of ROIs showed the expected language response (see Figure 4). The frontal pole and the more anterior superior frontal gyrus ROIs did not respond to linguistic content. In line with the main analysis, pseudosentences and sentences showed the highest percent signal changes and, generally, the strongest evidence in favor of the alternative hypothesis (percent signal change  $>0$ ).

**TABLE 2** ROI statistics for the language network

Brain region	Task main effect			Linear contrast		
	$F_{4, 60}$	$p$	$n_p^2$	$F_{1,15}$	$p$	$n_p^2$
L posterior middle temporal gyrus	22.72	<.001	.60	36.39	<.001	.71
L inferior frontal gyrus, pars triangularis	15.01	<.001	.50	42.77	<.001	.74
L middle temporal gyrus	18.69	<.001	.56	29.21	<.001	.66
L posterior supramarginal gyrus	24.59	<.001	.62	70.44	<.001	.82
L inferior frontal gyrus, pars opercularis	16.87	<.001	.53	27.40	<.01	.65
L temporal pole	6.63	<.01	.31	17.89	<.01	.54
Superior frontal gyrus	7.71	.001	.34	20.71	<.01	.58
Superior frontal gyrus	3.88	.087	—	3.78	.85	—
R posterior superior temporal gyrus	20.49	<.001	.58	45.81	<.001	.75
Frontal pole	5.20	.014	.26	8.25	.14	—
L middle frontal gyrus	6.93	<.01	.32	13.09	.03	.47
R temporal pole	5.28	.012	.26	19.77	<.01	.57

Note:  $p$  values are Bonferroni corrected for the number of comparisons ( $\alpha = .05/12$  ROIs). Labels taken from the Harvard-Oxford cortical atlas.

Abbreviations: L, Left; R, Right; ROI, region-of-interest.

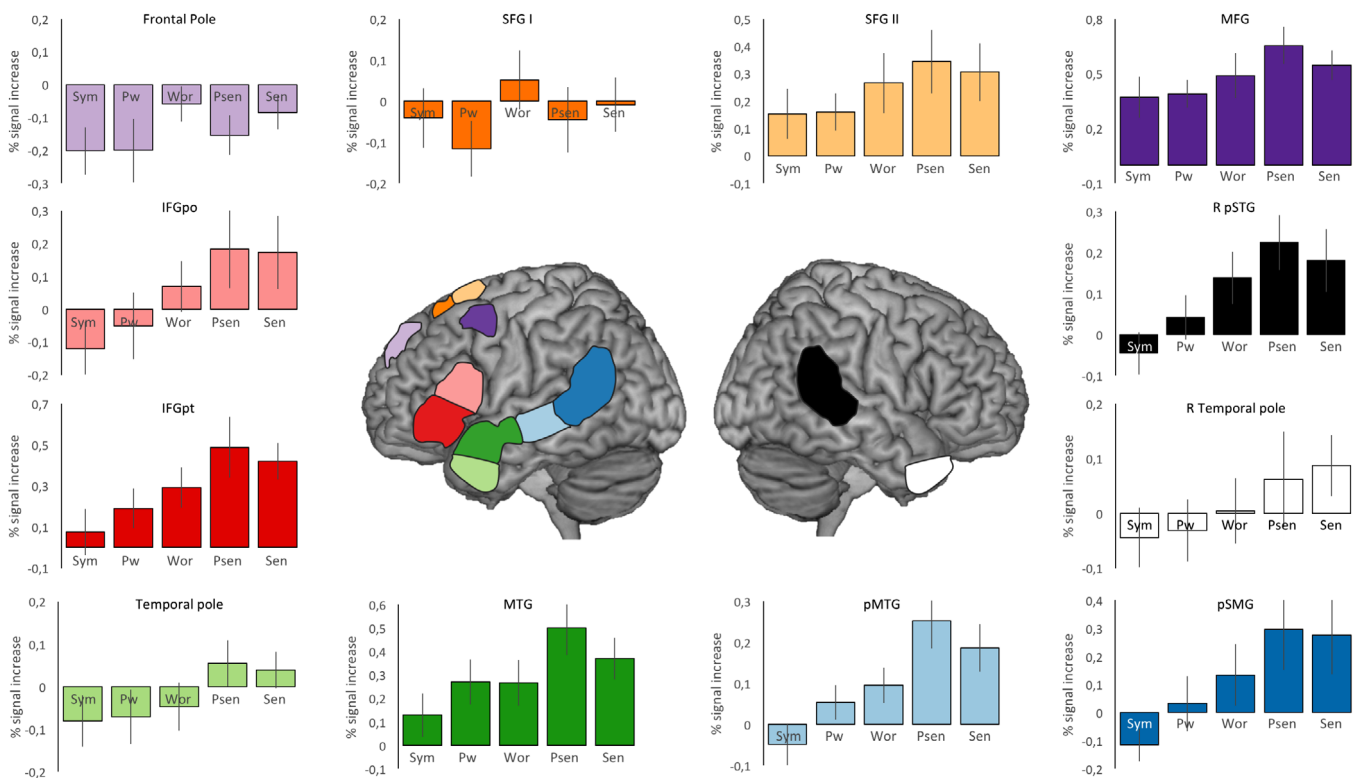


**FIGURE 4** Mean percent signal changes for each condition, for each of the 12 region-of-interests (ROIs) used to examine the language network. Bar graphs are color-coded in respect to each ROI in the center figure. Vertical bars denote 95% confidence intervals. Psen, pseudosentences; Pwor, pseudowords; Sen, sentences; Sym, symbols; Wor, words. Vertical bars denote 95% confidence intervals

### 3.4 | Single-subject results

Considering the relevance of rsfMRI for presurgical planning, we wanted to explore whether group-level results would be replicable at

the single-subject level. As for the group-level analyses, a repeated-measures ANOVA was calculated including the single-subject percent signal changes of the five conditions in a single within-subjects factor, Task. Again, a main effect of task was observed ( $F(4, 60) = 9.792$ ,

$p < .001$ ,  $\eta_p^2 = .40$ ). Bonferroni posthoc tests showed that pseudosentences and sentences elicited higher percent signal changes than symbols ( $p = .008$  and  $.048$ , respectively) and pseudowords ( $p < .001$  and  $p = .025$ , respectively). Words showed higher percent signal changes than pseudowords ( $p = .025$ ), and words, sentences and pseudosentences did not differ significantly from each other (all  $p_s > .58$ ). More importantly, we tested for linear effects in the linguistic conditions and found a significant linear model fit,  $F(1, 15) = 23.02$ ,  $p < .001$ ,  $\eta_p^2 = .61$ , with results following the same linear trend as observed for group-level results: more linguistic content corresponded to higher percent signal changes. Considering now the evidence in favor of significant activity during task execution (percent signal change  $>0$ ), symbols and pseudowords showed moderate evidence in favor of the null hypothesis (percent signal change  $>0$ ), with  $BF_{+0}$  of 0.34 and 0.35, respectively, whereas higher-level linguistic stimuli showed decisive evidence in favor of the alternative hypothesis, with  $BF_{+0}$  of 283.98, 139.16 and 219.42 for words, pseudosentences and sentences, respectively.

### 3.5 | Network specificity

We further examined whether the group-level language-responsive profile was restricted to the language network or whether it was also observed in other well-established networks. To do so, we calculated percent signal changes within three additional networks: the FPN, the DMN, and the DAN network. A  $5 \times 4$  repeated-measures ANOVA was calculated with within-subject factors Task (symbols, pseudowords, words, pseudosentences and sentences) and Network (Language, FPN, DMN, and DAN). To test the linear language-specific response across conditions, we ran a linear contrast for the factor Task, and a simple contrast for the factor Network (language vs. each other network). We observed a Task  $\times$  Network interaction ( $F(12, 180) = 13.46$ ,  $p < .001$ ,  $\eta_p^2 = .47$ ). Within-subject contrasts showed that the language network had a significantly higher linear model fit than the other networks (interactions Task  $\times$  Network,  $F_s > 28.8$ ,  $p_s < .001$ ,  $\eta_p^2 > .66$ ).

For completeness, we also examined task effects for each network separately to test for the presence of linear effects within the FPN, DMN, and DAN networks. The FPN network did not show significant differences between conditions ( $F(4, 60) = 2.07$ ,  $p = .095$ , *ns*) and generally was not recruited by the task (low to negligible percent signal change). The DMN also did not show statistically significant differences between conditions ( $F(4, 60) = 2.44$ ,  $p = .056$ , *ns*). Despite the trend-level statistical significance, results were generally characterized by linear deactivation—all conditions elicited negative percent signal changes, and the less linguistic content, the lower the percent signal changes (see Figure 3). Finally, the DAN network showed a significant main effect of Task ( $F(4, 60)$ ,  $p < .001$ ,  $\eta_p^2 = .56$ ) and a significant linear fit ( $F(1, 15) = 40.00$ ,  $p < .001$ ,  $\eta_p^2 = .73$ ). This effect was in the opposite direction of the one found for language: conditions with less linguistic material had the highest percent signal changes.

### 3.6 | Voxelwise correlation between task results and rsfMRI

We further assessed whether rsfMRI was able to identify the same regional patterns that can be identified by task-based fMRI at a fine-grain level (voxelwise correlation). We first calculated the contrast sentences  $>$  pseudowords (e.g., Fedorenko et al., 2010), and used resulting maps as a language localizer. Then, to examine similarity in these fine-grain activity patterns, we performed a voxelwise correlation of the unthresholded maps for the language localizer and the rsfMRI language network. This was performed restricted to voxels within the language network, and for both group-level maps and single-subject maps. We found a moderate voxelwise correlation ( $r = .42$ ) at the group-level, and a poor voxelwise correlation (mean  $r = .27$ , 95% CI 17.8–36.2, range 0.01–0.6) in single-subject data, suggesting that the rsfMRI networks are not very efficient in capturing the same fine-grain patterns that are observed during task execution. The localizer maps alongside the resting-state networks for each subject can be inspected in the Figure S6. Localizer maps are additionally available in NeuroVault (<https://neurovault.org/collections/SARZAHAW>).

## 4 | DISCUSSION

The goal of the present work was to investigate the functional profile of the rsfMRI language network. To do so, we examined if brain regions mapped with rsfMRI were engaged in tasks and stimuli with increasingly higher linguistic content as compared to a non-linguistic baseline. Our findings can be summarized in three key points. First, the language network responded selectively to linguistic involvement, with higher linguistic content leading to higher percent signal changes. This response pattern was observed for the majority of ROIs within the network, which suggests that this network subtends high-level language processing. Second, selective responses to linguistic content were also found at the single-subject level, attesting the feasibility of this procedure for single-subject mapping. Third, other networks previously linked to language processing did not respond to, nor were modulated by, language complexity, and thus are not directly linked to language processing; they probably tap domain-general processes that subtend task execution. Taken together, the above findings demonstrate that maps extracted with rsfMRI identify linguistically-relevant regions in the brain. This holds promise for applications of rsfMRI to study language processes in participants with poor task performance.

In this study, we used a multi-level experimental design to determine if regions within the network responded predominantly to language-rich conditions, as should be the case if they play a key linguistic role (Bedny et al., 2011; Fedorenko et al., 2016). The language network as a whole showed significant percent signal changes in conditions with linguistic content, and was characterized by a linear trend whereby higher linguistic content led to larger percent signal changes. Further, a comparison between conditions also

showed that sentences and pseudosentences had higher percent signal changes when compared to words, pseudowords and symbols. Considering that sentences combine three aspects of language—phonology, semantics and syntax (Hagoort, 2014; Hickok & Poeppel, 2007)—this finding was expected, and we interpret it as a correlate of the increased linguistic demands of sentences in comparison to words. This response pattern was also observed in previous studies (Fedorenko et al., 2010; Fedorenko et al., 2016). In contrast, symbols (the nonlinguistic baseline) did not elicit significant percent signal changes; instead they show moderate evidence in favor of the null hypothesis (percent signal changes equal or lower than zero). This effectively rules out the possibility that the language network was solely supporting domain-general processes (e.g., memory, attention) recruited by the probe-detection task used in this study.

Sentences and pseudosentences showed equivalent percent signal changes from baseline. This result is somewhat surprising because even though both have similar syntactic and phonological characteristics, the pseudosentences lack semantic content. It also stands at odds with previous findings showing that in a similar probe-detection task sentences elicit larger percent signal changes than pseudosentences in language-specific ROIs (Bedny et al., 2011). One possible explanation of this result is the predictability of the experimental material used here. Even though subjects were explicitly instructed to avoid using other strategies during task performance, as pseudosentences were generated by replacing content words with pseudowords while keeping function words intact, it could be that subjects retrieved some meaning even in the absence of content words. In fact, in the post-experiment survey two subjects reported that as the “sentence” was somehow right (it respected syntactic structure) they tended to unintentionally fill in the gaps and make some sense of it. With this in mind, it is worth pointing out that pseudosentences showed the highest variability out of all conditions (almost twice as large as in the sentence condition, see confidence intervals in Figure 3(a)), a result which could hint at the use of different strategies across subjects. As a consequence of this variability and despite the fact that pseudosentences had the absolute highest percent signal change, it was sentences that had the highest statistical power and evidence in favor of the alternative hypothesis (percent signal change  $>0$ ), Bayes factors ( $BF_{+0}$ ) of 840,668 versus 66,598 for pseudosentences.

To complement the findings observed at the network level, we examined the response patterns in a set of ROIs derived from the rsfMRI language network. Similarly to the main results, the majority of ROIs within the language network showed a language-sensitive response, higher linguistic content eliciting larger brain responses. These ROIs include brain regions consistently reported in the literature as language-related; more specifically, the inferior frontal gyrus pars triangularis and opercularis (also known as Broca's area), the middle frontal gyrus, posterior regions of the superior and middle temporal gyri (also known as Wernicke's area), and temporal regions including the superior temporal sulcus and the anterior temporal lobe (Jackson et al., 2016; Price, 2012). While the exact functional role

subtending each ROI is outside the scope of this manuscript, the linear trend of higher linguistic content leading to larger percent signal changes was found for most of the language-sensitive ROIs. Some studies emphasize specific computations in some of these ROIs. For instance, a main involvement of the IFG in syntactic processing (Friederici, 2002; Segaert, Menenti, Weber, Petersson, & Hagoort, 2011; Tyler et al., 2011) and the involvement of the posterior MTG for lexical access (Davey et al., 2016; Hickok & Poeppel, 2007). We did not, however, find evidence of this regional specificity. Our results instead accord well with studies comparing low-level to high-level linguistic material (Fedorenko et al., 2016), where language-rich conditions elicit larger responses than language-poor conditions, such as pseudowords and pseudosentences, in several frontal and temporal ROIs. In line with these results are recent demonstrations that syntactic processing is distributed over the whole language network (Blank & Fedorenko, 2017).

The resting-state language network also mapped other less established language-related brain regions, namely dorsal brain regions including the superior frontal gyrus extending into the pre-SMA, and the frontal pole. The involvement of these regions in language processing has been previously noted, although not consistently (Price, 2012). It is not surprising that these regions were mapped using functional connectivity, considering the strong underlying structural connectivity between these dorsal regions and the inferior frontal gyrus via the frontal aslant tract (Catani et al., 2013; Dick, Garic, Graziano, & Tremblay, 2018). Still, these regions showed moderate to no involvement in our task. Can we take this as evidence that they do not play a role in language processing? Probably not. While we tried to capture several key language processes in our protocol, not all language-related processes were assessed. Speech production, motor planning, auditory feedback and prosody were left out of this protocol due to time constraints. Interestingly, these dorsal regions extending into the pre-SMA and SMA have been suggested to play a part in auditory perception, imagery and motor control for speech (Hickok & Poeppel, 2007; Lima et al., 2016; Price, 2012). Thus it is quite likely that our task-based protocol was not sensitive enough to capture them. Even so, it is remarkable that these two non-responsive ROIs represented only a small part of the language network (11% of all voxels within the language network). The vast majority of the network showed a clear language-specific profile.

An important question to address is whether the rsfMRI language network is able to map language efficiently and with good sensitivity at the single-subject level—the end goal of rsfMRI mapping in clinical settings. This is so because group-level results tend to smooth over individual differences that could be relevant in the context of single-subject mapping (Fedorenko et al., 2010). In this study, and to circumvent this limitation, we also examined task-based responses in single-subject data in subject-specific ROIs, extracted independently for each subject. The language rsfMRI networks were efficiently mapped for all subjects, were quite similar to the language network template, and mapped conventional language regions. This is yet another demonstration that rsfMRI is able to

map the language network in the brain of single-subjects, in line with previous studies (Branco et al., 2016; Sair et al., 2016; Tie et al., 2014). Also, the single-subject language networks were specifically engaged in language, showing a similar pattern to that observed in the group-level results: sentences and pseudosentences elicited larger percent signal changes than symbols, pseudowords and words, and higher linguistic demands lead to larger percent signal changes. To our knowledge, this is the first demonstration that the language network, as extracted with ICA, is able to recruit regions that are linguistically relevant at the single-subject level and thus can be used to map language efficiently, including high-level brain regions implicated in syntactic and semantic processing. It is worth pointing out, though, that despite finding consistent responses within the inferior frontal gyrus and the middle temporal lobe (mapped in the majority of subjects, see Figure 2(b)), resting-state maps can be quite variable across subjects in other brain regions including the anterior temporal lobe, the middle frontal gyrus and the inferior temporal gyrus. Whether this reflects a limitation of the technique, or rather a subject-specific language topography, is not clear and should be studied in the future. Finally, although regions within the rsfMRI language network seem to respond to language complexity, it should be noted that the local patterns identified by rsfMRI match poorly to those identified by a conventional task-based localizer. It is well described that the language rsfMRI network and its task-based homolog overlap only partially (Branco et al., 2016; Tie et al., 2014), so this result is not unexpected. Causal studies using TMS and invasive brain stimulation are required to provide a more definite answer as to whether the mismatch between task-based and rsfMRI language maps proves clinically relevant.

There is currently conflicting evidence as to whether the language network is sufficient for language processing or whether other networks also play a role. In the latter case, it is crucial to examine what role exactly: is it language-specific or is it confounded by domain-general cognitive demands? We examined the three networks that have been associated to language processing, the left FPN, DMN and DAN networks. The FPN plays an important role for executive functions (e.g., Seeley et al., 2007). Considering our simple memory task, we did not expect marked increases in percent signal changes for this network. On the other hand, some studies have suggested that the left FPN plays a role in language, as regions within the network are recruited by tasks tapping into language and cognition (Laird et al., 2011; Smith et al., 2009). In our study, the left FPN did not respond to the task nor to increasing linguistic content. This finding suggests that the recruitment of the left FPN for language-related processes might be due to task-related executive demands. Whether FPN would show a language-characteristic response in tasks involving more active manipulation of linguistic stimuli is an open question that requires further study. The DMN is often referred to as the task-negative network (Biswal et al., 2010; Fox et al., 2005; Shehzad et al., 2009), and so we expected it to show negative percent signal changes, with higher activity during rest epochs as compared to task epochs. Unsurprisingly, the DMN showed a general deactivation for all

conditions and, consistent with previous studies (Binder et al., 2005; Humphries et al., 2007), a (non-significant, trend-level) linear pattern similar to that of language: conditions with higher linguistic content were less deactivated than those with weaker content. Hence, one should not to discard the idea that the DMN and the language networks interact dynamically over the course of task execution (Seghier & Price, 2012; Simony et al., 2016)—in this case, by showing less deactivation when linguistic demands are higher. Finally, we examined the DAN, a network recruited in tasks requiring sustained attention. Considering the nature of our task, we expected generally high percent signal changes irrespective of condition. On the other hand, this network should not be modulated by linguistic content (Fedorenko, 2014) but instead by task-demands, with more demanding tasks showing higher percent signal changes. This was exactly what we observed: all conditions elicited an overall positive and significant involvement in the task, and the condition with the highest percent signal change was the symbols condition—the non-linguistic baseline, which was also consistently the hardest condition (in accuracy, reaction times and also self-rated difficulty). This is strongly indicative of supra-modal, domain-general processing, in line with the idea that these regions stand side by side with language regions but do not track linguistic input (Blank & Fedorenko, 2017; Fedorenko et al., 2016). Taken together, these results show that the language network is highly specific and this language-specific response is not better explained by any other network other than the language network.

In this work, we show how language is efficiently mapped with rsfMRI in healthy subjects. It becomes now necessary to translate this knowledge to clinical settings, as the impact of pathology in resting-state functional connectivity is not yet fully understood. Previous evidence suggests that rsfMRI is able to map language in epilepsy and tumor patients (Branco et al., 2016; Sair et al., 2016), but it is likely that damage in large tracts such as the aslant and arcuate fasciculi, or damage in connectivity hubs, may impact functional connectivity (e.g., Gratton, Nomura, Pérez, & D'Esposito, 2012), potentially leading to poor mapping results. Further, although rsfMRI has great potential to capture plastic changes triggered by pathology (Hartwigsen & Saur, 2019; Klingbeil, Wawrzyniak, Stockert, & Saur, 2019), there are many open questions that need to be answered: can rsfMRI map these changes over time? Can rsfMRI be used to predict outcomes, or used to guide treatment? In summary, despite the promising progress in brain mapping using rsfMRI, and its novel applications in the clinical setting such as presurgical planning, further research is needed, and caution is warranted before generalizing these findings to the clinical realm.

This study has some limitations. Due to time restrictions and to avoid subject fatigue during the scanning session, we only included one task and five conditions in the experimental protocol. Lower-level perceptual processes (including speech perception and visual letter recognition), motor processes (speech articulation or hand motor control in writing/typing), and prosody perception / production were not investigated in the current paradigm. Ideally, studies employing more diverse language tasks should be performed to better gauge the

specificity and sensitivity of rsfMRI for language mapping. Also, the order of the experimental conditions was counterbalanced across subjects, but not within-subjects. Half of the subjects viewed, for example, symbols first, then pseudowords, and vice-versa, but each run had only one stimulus type and this could have influenced the percent signal changes across conditions; some of the ROIs within the language rsfMRI network, namely the left and right anterior temporal lobe, had signal loss that could have diminished the sensitivity and magnitude of the language response. Another limitation is that we employed a data-driven approach (ICA) to extract the language networks, and in the future it will be important to examine language responses of the language network as extracted through other methods including seed-based correlation (Smitha, Arun, Rajesh, Thomas, & Kesavadas, 2017) or artificial neural networks (e.g., Mitchell et al., 2013). Finally, we did not examine how the language network dynamically responded to linguistic information, and how it interacted with the other networks. This could provide important clues regarding the functional connectivity profile underlying language processing and its relationship with other networks. We will pursue this goal in the future.

## 5 | CONCLUSION

In summary, we examined the functional profile of the language rsfMRI network with a multi-level language protocol tapping into low- and high-level linguistic processes. We have shown that brain responses within the language network are modulated by linguistic content, a result that strongly suggests that this network is critical for language processing. This pattern emerged not only in group-level analyses, but also in single-subject data, and was evident in the majority of the regions of interest within the network. Importantly, these responses were only observed for the language network; other rsfMRI networks did not show a language-specific profile. Taken together, these results show that the language resting-state network can account for key language processes that are of utmost importance in the context of mapping eloquent functions in clinical settings, with important implications for presurgical planning. This strengthens the view that resting-state fMRI is a suitable technique for language mapping and can be used to complement—and potentially replace—task-based fMRI approaches for language mapping.

## DATA AVAILABILITY STATEMENT

The data that support the findings of this study are available from the corresponding author upon reasonable request.

## ORCID

Paulo Branco  <https://orcid.org/0000-0002-9425-046X>  
 São L. Castro  <https://orcid.org/0000-0002-1487-3596>

## REFERENCES

- Andersson, J. L., Jenkinson, M., & Smith S. (2007). *Non-linear Registration, Aka Spatial Normalization*. FMRIB Technical Report TR07JA2. Retrieved from [www.fmrib.ox.ac.uk/analysis/techrep](http://www.fmrib.ox.ac.uk/analysis/techrep)
- Beckmann, C., DeLuca, M., Devlin, J., & Smith, S. (2005). Investigations into resting-state connectivity using independent component analysis. *Philosophical Transactions of the Royal Society B: Biological Sciences*, 360(1457), 1001–1013. <https://doi.org/10.1098/rstb.2005.1634>
- Beckmann, C., & Smith, S. (2004). Probabilistic independent component analysis for functional magnetic resonance imaging. *IEEE Transactions on Medical Imaging*, 23(2), 137–152. <https://doi.org/10.1109/tmi.2003.822821>
- Bedny, M., Pascual-Leone, A., Dodell-Feder, D., Fedorenko, E., & Saxe, R. (2011). Language processing in the occipital cortex of congenitally blind adults. *Proceedings of the National Academy of Sciences*, 108(11), 4429–4434. <https://doi.org/10.1073/pnas.1014818108>
- Binder, J., Desai, R., Graves, W., & Conant, L. (2009). Where is the semantic system? A critical review and meta-analysis of 120 functional neuroimaging studies. *Cerebral Cortex*, 19(12), 2767–2796. <https://doi.org/10.1093/cercor/bhp055>
- Binder, J., Frost, J., Hammeke, T., Cox, R., Rao, S., & Prieto, T. (1997). Human brain language areas identified by functional magnetic resonance imaging. *The Journal of Neuroscience*, 17(1), 353–362. <https://doi.org/10.1523/jneurosci.17-01-00353.1997>
- Binder, J., Medler, D., Desai, R., Conant, L., & Liebenthal, E. (2005). Some neurophysiological constraints on models of word naming. *NeuroImage*, 27(3), 677–693. <https://doi.org/10.1016/j.neuroimage.2005.04.029>
- Binder, J., Swanson, S., Hammeke, T., & Sabsevitz, D. (2008). A comparison of five fMRI protocols for mapping speech comprehension systems. *Epilepsia*, 49(12), 1980–1997. <https://doi.org/10.1111/j.1528-1167.2008.01683.x>
- Biswal, B., Mennes, M., Zuo, X., Gohel, S., Kelly, C., Smith, S., ... Milham, M. P. (2010). Toward discovery science of human brain function. *Proceedings of the National Academy of Sciences*, 107(10), 4734–4739. <https://doi.org/10.1073/pnas.0911855107>
- Biswal, B., Zerrin Yetkin, F., Haughton, V., & Hyde, J. (1995). Functional connectivity in the motor cortex of resting human brain using echo-planar mri. *Magnetic Resonance in Medicine*, 34(4), 537–541. <https://doi.org/10.1002/mrm.1910340409>
- Blank, I., & Fedorenko, E. (2017). Domain-general brain regions do not track linguistic input as closely as language-selective regions. *The Journal of Neuroscience*, 37(41), 9999–10011. <https://doi.org/10.1523/jneurosci.3642-16.2017>
- Bookheimer, S. (2007). Pre-surgical language mapping with functional magnetic resonance imaging. *Neuropsychology Review*, 17(2), 145–155. <https://doi.org/10.1007/s11065-007-9026-x>
- Brainard, D. (1997). The psychophysics toolbox. *Spatial Vision*, 10(4), 433–436. <https://doi.org/10.1163/156856897x00357>
- Branco, P., Seixas, D., & Castro, S. (2018). Temporal reliability of ultra-high field resting-state MRI for single-subject sensorimotor and language mapping. *NeuroImage*, 168, 499–508. <https://doi.org/10.1016/j.neuroimage.2016.11.029>
- Branco, P., Seixas, D., Deprez, S., Kovacs, S., Peeters, R., Castro, S., & Sunaert, S. (2016). Resting-state functional magnetic resonance imaging for language preoperative planning. *Frontiers in Human Neuroscience*, 10, 11. <https://doi.org/10.3389/fnhum.2016.00011>
- Castro, S., & Lima, C. (2010). Recognizing emotions in spoken language: A validated set of Portuguese sentences and pseudosentences for research on emotional prosody. *Behavior Research Methods*, 42(1), 74–81. <https://doi.org/10.3758/brm.42.1.74>
- Catani, M., Mesulam, M., Jakobsen, E., Malik, F., Martersteck, A., Wieneke, C., ... Rogalsky, E. (2013). A novel frontal pathway underlies

- verbal fluency in primary progressive aphasia. *Brain*, 136(8), 2619–2628. <https://doi.org/10.1093/brain/awt163>
- Damoiseaux, J., Rombouts, S., Barkhof, F., Scheltens, P., Stam, C., Smith, S., & Beckmann, C. (2006). Consistent resting-state networks across healthy subjects. *Proceedings of the National Academy of Sciences*, 103(37), 13848–13853. <https://doi.org/10.1073/pnas.0601417103>
- Davey, J., Thompson, H., Hallam, G., Karapanagiotidis, T., Murphy, C., De Caso, I., ... Jefferies, E. (2016). Exploring the role of the posterior middle temporal gyrus in semantic cognition: Integration of anterior temporal lobe with executive processes. *NeuroImage*, 137, 165–177. <https://doi.org/10.1016/j.neuroimage.2016.05.051>
- Deco, G., Jirsa, V., & McIntosh, A. (2011). Emerging concepts for the dynamical organization of resting-state activity in the brain. *Nature Reviews Neuroscience*, 12(1), 43–56. <https://doi.org/10.1038/nrn2961>
- Dick, A., Garic, D., Graziano, P., & Tremblay, P. (2018). The frontal aslant tract (FAT) and its role in speech, language and executive function. *Cortex*, 111, 148–163. <https://doi.org/10.1016/j.cortex.2018.10.015>
- Esposito, F., Aragri, A., Latorre, V., Popolizio, T., Scarabino, T., Cirillo, S., ... Di Salle, F. (2009). Does the default-mode functional connectivity of the brain correlate with working-memory performances? *Arch. Ital. Biol.*, 147, 11–20.
- Fedorenko, E. (2014). The role of domain-general cognitive control in language comprehension. *Frontiers in Psychology*, 5, 335. <https://doi.org/10.3389/fpsyg.2014.00335>
- Fedorenko, E., Duncan, J., & Kanwisher, N. (2012). Language-selective and domain-general regions lie side by side within Broca's area. *Current Biology*, 22(21), 2059–2062. <https://doi.org/10.1016/j.cub.2012.09.011>
- Fedorenko, E., Duncan, J., & Kanwisher, N. (2013). Broad domain generality in focal regions of frontal and parietal cortex. *Proceedings of the National Academy of Sciences*, 110(41), 16616–16621. <https://doi.org/10.1073/pnas.1315235110>
- Fedorenko, E., Hsieh, P., Nieto-Castañón, A., Whitfield-Gabrieli, S., & Kanwisher, N. (2010). New method for fMRI investigations of language: Defining ROIs functionally in individual subjects. *Journal of Neurophysiology*, 104(2), 1177–1194. <https://doi.org/10.1152/jn.00032.2010>
- Fedorenko, E., Scott, T., Brunner, P., Coon, W., Pritchett, B., Schalk, G., & Kanwisher, N. (2016). Neural correlate of the construction of sentence meaning. *Proceedings of the National Academy of Sciences*, 113(41), E6256–E6262. <https://doi.org/10.1073/pnas.1612132113>
- Fedorenko, E., & Thompson-Schill, S. (2014). Reworking the language network. *Trends in Cognitive Sciences*, 18(3), 120–126. <https://doi.org/10.1016/j.tics.2013.12.006>
- Fox, M., & Raichle, M. (2007). Spontaneous fluctuations in brain activity observed with functional magnetic resonance imaging. *Nature Reviews Neuroscience*, 8(9), 700–711. <https://doi.org/10.1038/nrn2201>
- Fox, M., Snyder, A., Vincent, J., Corbetta, M., Van Essen, D., & Raichle, M. (2005). From the cover: The human brain is intrinsically organized into dynamic, anticorrelated functional networks. *Proceedings of the National Academy of Sciences*, 102(27), 9673–9678. <https://doi.org/10.1073/pnas.0504136102>
- Friederici, A. (2002). Towards a neural basis of auditory sentence processing. *Trends in Cognitive Sciences*, 6(2), 78–84. [https://doi.org/10.1016/s1364-6613\(00\)01839-8](https://doi.org/10.1016/s1364-6613(00)01839-8)
- Geranmayeh, F., Chau, T., Wise, R., Leech, R., & Hampshire, A. (2017). Domain-general subregions of the medial prefrontal cortex contribute to recovery of language after stroke. *Brain*, 140(7), 1947–1958. <https://doi.org/10.1093/brain/awx134>
- Geranmayeh, F., Wise, R., Mehta, A., & Leech, R. (2014). Overlapping networks engaged during spoken language production and its cognitive control. *Journal of Neuroscience*, 34(26), 8728–8740. <https://doi.org/10.1523/jneurosci.0428-14.2014>
- Gratton, C., Nomura, E., Pérez, F., & D'Esposito, M. (2012). Focal brain lesions to critical locations cause widespread disruption of the modular organization of the brain. *Journal of Cognitive Neuroscience*, 24(6), 1275–1285. [https://doi.org/10.1162/jocn\\_a\\_00222](https://doi.org/10.1162/jocn_a_00222)
- Hagoort, P. (2014). Nodes and networks in the neural architecture for language: Broca's region and beyond. *Current Opinion in Neurobiology*, 28, 136–141. <https://doi.org/10.1016/j.conb.2014.07.013>
- Hartwigsen, G., & Saur, D. (2019). Neuroimaging of stroke recovery from aphasia – Insights into plasticity of the human language network. *NeuroImage*, 190, 14–31. <https://doi.org/10.1016/j.neuroimage.2017.11.056>
- Hertrich, I., Dietrich, S., & Ackermann, H. (2016). The role of the supplementary motor area for speech and language processing. *Neuroscience & Biobehavioral Reviews*, 68, 602–610. <https://doi.org/10.1016/j.neubiorev.2016.06.030>
- Hickok, G., & Poeppel, D. (2007). The cortical organization of speech processing. *Nature Reviews Neuroscience*, 8(5), 393–402. <https://doi.org/10.1038/nrn2113>
- Humphreys, G., & Lambon Ralph, M. (2014). Fusion and fission of cognitive functions in the human parietal cortex. *Cerebral Cortex*, 25(10), 3547–3560. <https://doi.org/10.1093/cercor/bhu198>
- Humphries, C., Binder, J., Medler, D., & Liebenthal, E. (2007). Time course of semantic processes during sentence comprehension: An fMRI study. *NeuroImage*, 36(3), 924–932. <https://doi.org/10.1016/j.neuroimage.2007.03.059>
- Jackson, R., Cloutman, L., & Lambon Ralph, M. (2019). Exploring distinct default mode and semantic networks using a systematic ICA approach. *Cortex*, 113, 279–297. <https://doi.org/10.1016/j.cortex.2018.12.019>
- Jackson, R., Hoffman, P., Pobric, G., & Lambon Ralph, M. (2016). The semantic network at work and rest: Differential connectivity of anterior temporal lobe subregions. *The Journal of Neuroscience*, 36(5), 1490–1501. <https://doi.org/10.1523/jneurosci.2999-15.2016>
- Jenkinson, M., Bannister, P., Brady, M., & Smith, S. (2002). Improved optimization for the robust and accurate linear registration and motion correction of brain images. *NeuroImage*, 17(2), 825–841. <https://doi.org/10.1006/nimg.2002.1132>
- Klingbeil, J., Wawrzyniak, M., Stockert, A., & Saur, D. (2019). Resting-state functional connectivity: An emerging method for the study of language networks in post-stroke aphasia. *Brain and Cognition*, 131, 22–33. <https://doi.org/10.1016/j.bandc.2017.08.005>
- Laird, A., Fox, P., Eickhoff, S., Turner, J., Ray, K., McKay, D., ... Fox, P. (2011). Behavioral interpretations of intrinsic connectivity networks. *Journal of Cognitive Neuroscience*, 23(12), 4022–4037. [https://doi.org/10.1162/jocn\\_a\\_00077](https://doi.org/10.1162/jocn_a_00077)
- Lima, C., Krishnan, S., & Scott, S. (2016). Roles of supplementary motor areas in auditory processing and auditory imagery. *Trends in Neurosciences*, 39(8), 527–542. <https://doi.org/10.1016/j.tins.2016.06.003>
- McKiernan, K., Kaufman, J., Kucera-Thompson, J., & Binder, J. (2003). A parametric manipulation of factors affecting task-induced deactivation in functional neuroimaging. *Journal of Cognitive Neuroscience*, 15(3), 394–408. <https://doi.org/10.1162/089892903321593117>
- Mitchell, T., Hacker, C., Breshears, J., Szrama, N., Sharma, M., Bundy, D., ... Leuthardt, E. C. (2013). A novel data-driven approach to preoperative mapping of functional cortex using resting-state functional magnetic resonance imaging. *Neurosurgery*, 73(6), 969–983. <https://doi.org/10.1227/neu.0000000000000141>
- Mumford, J., & Nichols, T. (2008). Power calculation for group fMRI studies accounting for arbitrary design and temporal autocorrelation. *NeuroImage*, 39(1), 261–268. <https://doi.org/10.1016/j.neuroimage.2007.07.061>
- Murphy, K., Bodurka, J., & Bandettini, P. (2007). How long to scan? The relationship between fMRI temporal signal to noise ratio and necessary scan duration. *NeuroImage*, 34(2), 565–574. <https://doi.org/10.1016/j.neuroimage.2006.09.032>

- Oldfield, R. (1971). The assessment and analysis of handedness: The Edinburgh inventory. *Neuropsychologia*, 9(1), 97–113. [https://doi.org/10.1016/0028-3932\(71\)90067-4](https://doi.org/10.1016/0028-3932(71)90067-4)
- Parker Jones, O., Voets, N., Adcock, J., Stacey, R., & Jbabdi, S. (2017). Resting connectivity predicts task activation in pre-surgical populations. *NeuroImage: Clinical*, 13, 378–385. <https://doi.org/10.1016/j.nicl.2016.12.028>
- Pillai, J., & Zaca, D. (2011). Relative utility for hemispheric lateralization of different clinical fMRI activation tasks within a comprehensive language paradigm battery in brain tumor patients as assessed by both threshold-dependent and threshold-independent analysis methods. *NeuroImage*, 54, S136–S145. <https://doi.org/10.1016/j.neuroimage.2010.03.082>
- Price, C. (2012). A review and synthesis of the first 20 years of PET and fMRI studies of heard speech, spoken language and reading. *NeuroImage*, 62, 816–847.
- Price, C., Crinion, J., & Friston, K. (2006). Design and analysis of fMRI studies with neurologically impaired patients. *Journal of Magnetic Resonance Imaging*, 23(6), 816–826. <https://doi.org/10.1002/jmri.20580>
- Pruim, R., Mennes, M., van Rooij, D., Llera, A., Buitelaar, J., & Beckmann, C. (2015). ICA-AROMA: A robust ICA-based strategy for removing motion artifacts from fMRI data. *NeuroImage*, 112, 267–277. <https://doi.org/10.1016/j.neuroimage.2015.02.064>
- Ralph, M., Jefferies, E., Patterson, K., & Rogers, T. (2016). The neural and computational bases of semantic cognition. *Nature Reviews Neuroscience*, 18(1), 42–55. <https://doi.org/10.1038/nrn.2016.150>
- Rombouts, S., Barkhof, F., Hoogenraad, F., Sprenger, M., & Scheltens, P. (1998). Within-subject reproducibility of visual activation patterns with functional magnetic resonance imaging using multislice Echo planar imaging. *Magnetic Resonance Imaging*, 16, 105–113.
- Sair, H., Yahyavi-Firouz-Abadi, N., Calhoun, V., Airan, R., Agarwal, S., Intrapromkul, J., ... Pillai, J. J. (2016). Presurgical brain mapping of the language network in patients with brain tumors using resting-state fMRI: Comparison with task fMRI. *Human Brain Mapping*, 37(3), 913–923. <https://doi.org/10.1002/hbm.23075>
- Saur, D., Kreher, B., Schnell, S., Kummerer, D., Kellmeyer, P., Vry, M., ... Weiller, C. (2008). Ventral and dorsal pathways for language. *Proceedings of the National Academy of Sciences*, 105(46), 18035–18040. <https://doi.org/10.1073/pnas.0805234105>
- Seeley, W., Menon, V., Schatzberg, A., Keller, J., Glover, G., Kenna, H., ... Greicius, M. D. (2007). Dissociable intrinsic connectivity networks for salience processing and executive control. *Journal of Neuroscience*, 27(9), 2349–2356. <https://doi.org/10.1523/jneurosci.5587-06.2007>
- Segaert, K., Menenti, L., Weber, K., Petersson, K., & Hagoort, P. (2011). Shared syntax in language production and language comprehension—An fMRI study. *Cerebral Cortex*, 22(7), 1662–1670. <https://doi.org/10.1093/cercor/bhr249>
- Seghier, M., & Price, C. (2012). Functional heterogeneity within the default network during semantic processing and speech production. *Frontiers in Psychology*, 3, 281. <https://doi.org/10.3389/fpsyg.2012.00281>
- Shehzad, Z., Kelly, A., Reiss, P., Gee, D., Gotimer, K., Uddin, L., ... Milham, M. P. (2009). The resting brain: Unconstrained yet reliable. *Cerebral Cortex*, 19(10), 2209–2229. <https://doi.org/10.1093/cercor/bhn256>
- Shirer, W., Ryali, S., Rykhlevskaia, E., Menon, V., & Greicius, M. (2011). Decoding subject-driven cognitive states with whole-brain connectivity patterns. *Cerebral Cortex*, 22(1), 158–165. <https://doi.org/10.1093/cercor/bhr099>
- Simmons, W., Reddish, M., Bellgowan, P., & Martin, A. (2009). The selectivity and functional connectivity of the anterior temporal lobes. *Cerebral Cortex*, 20(4), 813–825. <https://doi.org/10.1093/cercor/bhp149>
- Simony, E., Honey, C., Chen, J., Lositsky, O., Yeshurun, Y., Wiesel, A., & Hasson, U. (2016). Dynamic reconfiguration of the default mode network during narrative comprehension. *Nature Communications*, 7(1), 12141. <https://doi.org/10.1038/ncomms12141>
- Smirnov, D., Glerean, E., Lahnakoski, J., Salmi, J., Jääskeläinen, I., Sams, M., & Nummenmaa, L. (2014). Fronto-parietal network supports context-dependent speech comprehension. *Neuropsychologia*, 63, 293–303. <https://doi.org/10.1016/j.neuropsychologia.2014.09.007>
- Smith, S. (2002). Fast robust automated brain extraction. *Human Brain Mapping*, 17(3), 143–155. <https://doi.org/10.1002/hbm.10062>
- Smith, S., Fox, P., Miller, K., Glahn, D., Fox, P., Mackay, C., ... Beckmann, C. F. (2009). Correspondence of the brain's functional architecture during activation and rest. *Proceedings of the National Academy of Sciences*, 106(31), 13040–13045. <https://doi.org/10.1073/pnas.0905267106>
- Smith, S., Jenkinson, M., Woolrich, M., Beckmann, C., Behrens, T., Johansen-Berg, H., ... Matthews, P. (2004). Advances in functional and structural MR image analysis and implementation as FSL. *NeuroImage*, 23, S208–S219. <https://doi.org/10.1016/j.neuroimage.2004.07.051>
- Smitha, K., Arun, K., Rajesh, P., Thomas, B., & Kesavadas, C. (2017). Resting-state seed-based analysis: An alternative to task-based language fMRI and its laterality index. *American Journal of Neuroradiology*, 38(6), 1187–1192. <https://doi.org/10.3174/ajnr.a5169>
- Soares, A., Iriarte, Á., Almeida, J., Simões, A., Costa, A., França, P., ... Comesaña, M. (2014). Procura-PALavras (P-Pal): Uma nova medida de frequência lexical do português europeu contemporâneo. *Psicologia: Reflexão E Crítica*, 27(1), 110–123. <https://doi.org/10.1590/s0102-79722014000100013>
- Stippich, C., Rapps, N., Dreyhaupt, J., Durst, A., Kress, B., Nennig, E., ... Sartor, K. (2007). Localizing and lateralizing language in patients with brain tumors: Feasibility of routine preoperative functional MR imaging in 81 consecutive patients. *Radiology*, 243(3), 828–836. <https://doi.org/10.1148/radiol.2433060068>
- Sunaert, S. (2006). Presurgical planning for tumor resectioning. *Journal of Magnetic Resonance Imaging*, 23(6), 887–905. <https://doi.org/10.1002/jmri.20582>
- Tavor, I., Jones, O., Mars, R., Smith, S., Behrens, T., & Jbabdi, S. (2016). Task-free MRI predicts individual differences in brain activity during task performance. *Science*, 352(6282), 216–220. <https://doi.org/10.1126/science.aad8127>
- Tie, Y., Rigolo, L., Norton, I., Huang, R., Wu, W., Orringer, D., ... Golby, A. (2014). Defining language networks from resting-state fMRI for surgical planning—a feasibility study. *Human Brain Mapping*, 35(3), 1018–1030. <https://doi.org/10.1002/hbm.22231>
- Tremblay, P., & Dick, A. (2016). Broca and Wernicke are dead, or moving past the classic model of language neurobiology. *Brain and Language*, 162, 60–71. <https://doi.org/10.1016/j.bandl.2016.08.004>
- Turken, A., & Dronkers, N. (2011). The neural architecture of the language comprehension network: Converging evidence from lesion and connectivity analyses. *Frontiers in System Neuroscience*, 5, 1. <https://doi.org/10.3389/fnsys.2011.00001>
- Tyler, L., Marslen-Wilson, W., Randall, B., Wright, P., Devereux, B., Zhuang, J., ... Stamakis, E. A. (2011). Left inferior frontal cortex and syntax: Function, structure and behaviour in patients with left hemisphere damage. *Brain*, 134(2), 415–431. <https://doi.org/10.1093/brain/awq369>
- Vidal, C., Content, A., & Chetail, F. (2017). BACS: The Brussels artificial character sets for studies in cognitive psychology and neuroscience. *Behavior Research Methods*, 49(6), 2093–2112. <https://doi.org/10.3758/s13428-016-0844-8>
- Vossel, S., Geng, J., & Fink, G. (2013). Dorsal and ventral attention systems. *The Neuroscientist*, 20(2), 150–159. <https://doi.org/10.1177/1073858413494269>
- Wagenmakers, E., Love, J., Marsman, M., Jamil, T., Ly, A., Verhagen, J., ... Morey, R. (2017). Bayesian inference for psychology. Part II: Example applications with JASP. *Psychonomic Bulletin & Review*, 25(1), 58–76. <https://doi.org/10.3758/s13423-017-1323-7>
- Whitfield-Gabrieli, S., & Nieto-Castanon, A. (2012). Conn: A functional connectivity toolbox for correlated and anticorrelated brain networks. *Brain Connectivity*, 2(3), 125–141. <https://doi.org/10.1089/brain.2012.0073>
- Wilson, S., Bautista, A., Yen, M., Lauderdale, S., & Eriksson, D. (2017). Validity and reliability of four language mapping paradigms.

*Neuroimage: Clinical*, 16, 399–408. <https://doi.org/10.1016/j.nicl.2016.03.015>

Woolrich, M., Behrens, T., Beckmann, C., & Smith, S. (2005). Mixture models with adaptive spatial regularization for segmentation with an application to FMRI data. *IEEE Transactions on Medical Imaging*, 24(1), 1–11. <https://doi.org/10.1109/tmi.2004.836545>

Zhang, Y., Brady, M., & Smith, S. (2001). Segmentation of brain MR images through a hidden Markov random field model and the expectation-maximization algorithm. *IEEE Transactions on Medical Imaging*, 20(1), 45–57. <https://doi.org/10.1109/42.906424>

Zhu, D., Chang, J., Freeman, S., Tan, Z., Xiao, J., Gao, Y., & Kong, J. (2014). Changes of functional connectivity in the left frontoparietal network following aphasic stroke. *Frontiers in Behavioral Neuroscience*, 8, 167. <https://doi.org/10.3389/fnbeh.2014.00167>

## SUPPORTING INFORMATION

Additional supporting information may be found online in the Supporting Information section at the end of this article.

**How to cite this article:** Branco P, Seixas D, Castro SL. Mapping language with resting-state functional magnetic resonance imaging: A study on the functional profile of the language network. *Hum Brain Mapp*. 2020;41:545–560. <https://doi.org/10.1002/hbm.24821>